FRP REINFORCEMENT OF WOOD ELEMENTS UNDER BENDING LOADS

Prof A. Borri, Dr M Corradi, Andrea Grazini
University of Perugia
Dept of Civil & Environmental Engineering
School of Engineering,
Via Duranti, 93
06125 Perugia, Italy
borri@unipg.it ; mcorradi@strutture.unipg.it ; agrazini@strutture.unipg.it

KEYWORDS: FRP, Wood, bending loads

ABSTRACT
This paper presents a study on the reinforcement of existing wood elements under bending loads through the use of FRP materials. First, an analytical investigation was conducted on the behavior of a generic FRP-reinforced wood section. This study, in turn, led to a numerical procedure based on non-linear wood properties, suitable for application in the design of FRP reinforcement of old, pre-existing wood beams under differing configurations of intervention layout and materials applied. At the end of this paper results of an experimental campaign are presented and used for comparison with the numerical procedure.

1. INTRODUCTION

Wood is a very efficient material. Its notable resistance under both compressive and traction loads becomes nearly unique if compared with its limited weight density.
However, due to its characteristics, this material has never been known for its durability. Wood elements used to bear bending loads, such as beams in the past, have been usually subjected either to replacement or reinforcement with classic techniques involving the use of common building materials such as concrete or steel.
During these last decades wood elements have been reinforced using various techniques, few of which have been successfully commercialized.
Nevertheless, some of these techniques have been used to consolidate existent wood beams where it is not possible to operate, for various reasons, a complete replacement of the wood element. In this perspective the introduction of composite materials as reinforcements for wood elements subjected to bending loads (Borri et al., 2001) or shear loads (Triantafillou, 1997) is of great interest. This interest is enhanced by the continuous progress made in FRP materials, together with their wider availability in different materials and shapes. Elements in wood, due to the nature of the material, can be subjected to a reinforcement intervention for several reasons: increment of dead loads, degradation of the mechanical properties of the element or the reduction of excessive displacements.
Specifically, the use of composite materials as a reinforcement for wood elements under bending loads requires particular attention to several aspects of the problem. First, it is very important to carefully plan the kind of intervention to be realized. In fact, there are many techniques (figure 1) of reinforcing a wood element using different layouts of the FRP elements and each choice could potentially lead to different results. When the choice has been made, the next step is the selection of the most adequate FRP elements. The wide range of products and the mechanical properties of FRP elements currently available can lead to a difficulty in choice for the designer who approaches this reinforcement technique.
For this reason, selection of the reinforcement should be guided by an accurate analysis of the characteristic of the element to reinforce in order to avoid ineffective interventions.

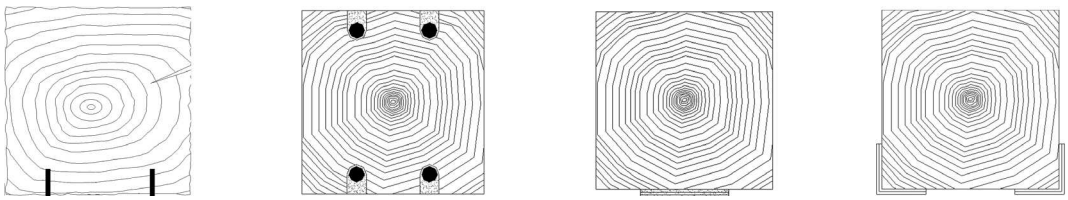

Figure 1 FRP reinforcement layouts on a wood section.

2. STUDY OF THE REINFORCEMENT

The calculation of bending loads for wood elements is usually conducted by mean of simplified approaches based on classic linear analysis, similarly to what is done for steel elements. On the one hand, this approach allows a quick and consistent evaluation of the current stress state of the wood element while, on the other hand, it does not take into account the non-linear behaviour that a wood element can exhibit, either with or without reinforcements.

2.1 Linear Analysis

The analysis of the tensional state caused by a bending moment acting on a wood element can be obtained through the equation :

$$\sigma_l = \pm \frac{M_s}{C \cdot W} \tag{1}$$

where M_s is the bending moment on the element, W is the section module and C is a coefficient that takes into account the timber quality. This approach can be directly applied to obtain stresses in the reinforced element using the equivalent section modulus W_e.
This value can be obtained through the coefficient n as follows:

$$n = \frac{E_{frp}}{E_l} \tag{2}$$

where E_{frp} is the Young modulus of the FRP and E_l is the Young wood modulus.
The n coefficient assumes values included between 10 and 40. However, this method does not represent the increments in terms of the stiffness and resistance in wood elements, as has been demonstrated in several experimental tests (Borri et al., 2001).
This difference is caused by the plasticization of the compressed region of the element, as shown in the simulation in figure 10. In this situation the plasticized region, despite contributing to the equilibrium of the element, does not contribute to the stiffness of the section. This increases the efficiency of the effect of the composite material, which is still working in the elastic phase. This is the reason for the importance of a non-linear analysis in the explanation of this behavior.

2.2 Non-Linear Analysis

Figure 2.a shows the layout assumed for the non-linear analysis. The numerical model takes into account the simultaneous presence of both upper and lower reinforcement on the section.
The stress-strain relationships assumed are the Bazan-Buchanan law (Bazan, 1980) for wood and a linear stress-strain law for composite materials. The Bazan-Buchanan law is characterized by an elastic-plastic line for compression and an elastic fragile line for tensile stresses. The choice of the parameters that describe the wood properties is very important in order to follow the actual behavior of the element under bending loads, particularly in order to carry out a limit analysis.

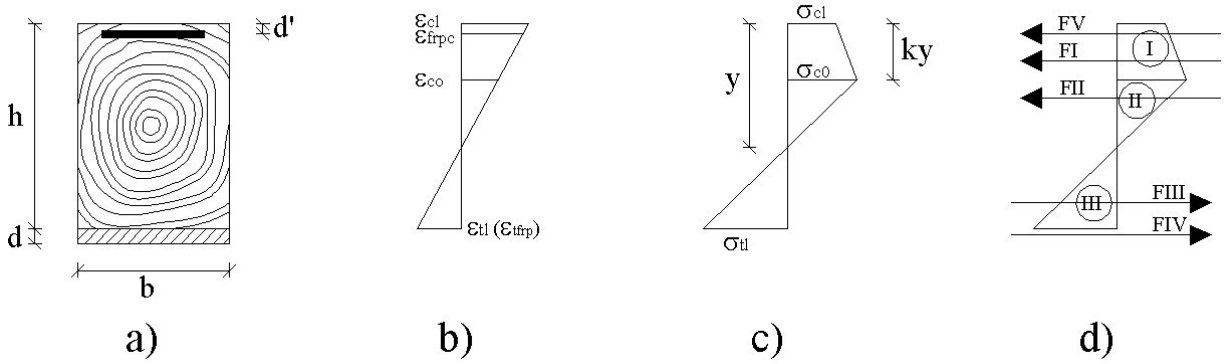

Figure 2 Ultimate limit scheme of a wood section.

Assuming the failure is not reached in the composite materials, it is possible to reduce the study of the problem to two failure cases (Triantafillou, 1991):

- Attainment of limit strain in compression region ε_{cu} without exceeding limit strain in the traction region.
- Attainment of limit strain in traction region ε_{tu} without exceeding limit strain in the compression region.

In both cases, from the condition of equilibrium it follows that:

$$F_I + F_{II} + F_V = F_{III} + F_{IV}\,, \tag{3}$$

where the forces in the compression region:

$$F_I = \frac{\sigma_{cl} + \sigma_{c0}}{2} \cdot b \cdot k \cdot y\,;\quad F_{II} = \frac{\sigma_{c0}}{2} \cdot b \cdot y \cdot (1-k);\quad F_V = A_{frpc} \cdot \sigma_{frpc} \tag{4}$$

and the forces in the tension zone:

$$F_{III} = \frac{\sigma_{tl}}{2} \cdot (h-y) \cdot b\,;\quad F_{IV} = A_{frpt} \cdot \sigma_{frpt} \tag{5}$$

where A_{frpt} represents the composite area in the traction region and A_{frpc} that in the compression region.
The preservation of plain sections, confirmed by several experimental results, will be assumed for the congruence equations.
Therefore:

$$\frac{\varepsilon_{cl}}{y} = \frac{\varepsilon_{tl}}{h-y} = \frac{\varepsilon_{c0}}{y(1-k)} = \frac{\varepsilon_{frpt}}{h+d-y} = \frac{\varepsilon_{frpc}}{y-d'} \tag{6}$$

From these equations and from the stress-strain laws of materials it is possible, for each failure case, to find the position of the neutral axis and the value of the ultimate bending moment of the section.
In particular, the Bazan-Buchanan law can be expressed as follows:

$$\begin{aligned} &\sigma_{cl} = E_l \cdot \varepsilon_{cl} && \text{se} \quad \varepsilon_{cl} < \varepsilon_{c0} \\ &\sigma_{cl} = \sigma_{c0} - m \cdot (\varepsilon_{cl} - \varepsilon_{c0}) && \text{se} \quad \varepsilon_{cl} > \varepsilon_{c0} \\ &\sigma_{tl} = E_l \cdot \varepsilon_{tl} \end{aligned} \tag{7}$$

Where *m* represents the slope of the plastic branch of the Bazan-Buchanan law.

$$m = \frac{\sigma_{c0} - \sigma_{cu}}{\varepsilon_{cu} - \varepsilon_{c0}} \tag{8}$$

The equations in (7) also take into account the possibility of having different elastic modules in traction and compression zones of the section.

In effect, preceding studies on the material indicate that in an overwhelming number of cases the difference between the two modules is almost negligible, respect to other simplifications assumed.
As regard FRP materials the generic stress-strain relationship will assume the following expressions:

$$\sigma_{frpc} = E_{frpc} \cdot \varepsilon_{frpc} \tag{9}$$

$$\sigma_{frpt} = E_{frpt} \cdot \varepsilon_{frpt} \tag{10}$$

which describe a linear elastic behaviour of the two materials.
Using equations (3)-(10) it is possible to find the neutral axis equation for each assumed failure case. If the failure is reached due to the complete plasticization of the compressed region with ultimate strain $\varepsilon_{cu,}$ then the neutral axis equation becomes:

$$\sigma_{c0} \cdot y^2 \cdot (1+\alpha-\alpha\delta) - E_l \cdot \varepsilon_{c0} \cdot (h-y)^2 + 2 \cdot \rho_{frpc} \cdot E_{frpc} \cdot b \cdot h \cdot \varepsilon_{cu} \cdot (y-d') - 2 \cdot \rho_{frpt} \cdot E_{frpt} \cdot h \cdot \varepsilon_{cu} \cdot (h+d-y) = 0 \tag{11}$$

where:

$$\alpha = \frac{\sigma_{cu}}{\sigma_{c0}} \; ; \quad \delta = \frac{\varepsilon_{c0}}{\varepsilon_{cu}} \; ; \tag{12}$$

are Bazan-Buchanan parameters and where:

$$\rho_{frpt} = \frac{A_{frpt}}{bh} \tag{13}$$

$$\rho_{frpc} = \frac{A_{frpc}}{bh} \tag{14}$$

are the area fractions for the two composite materials applied in the compression and traction areas.
Then, if the traction failure occurs, the neutral axis equation is expressed as follows:

$$y \cdot \left(2 \cdot \sigma_{c0} - \phi \cdot \left(\frac{\varepsilon_{tu} \cdot y}{h-y} - \varepsilon_{c0} \right) \right) + y \cdot \left(\varepsilon_{c0} \cdot \left(\frac{h-y}{\varepsilon_{tu} \cdot y} \right) \right) \cdot \left(\phi \cdot \left(\varepsilon_{tu} \cdot y / (h-y) - \varepsilon_{c0} \right) - \sigma_{c0} \right) -$$

$$- \sigma_{tu} \cdot (h-y) - 2 \cdot \rho_{frpt} \cdot (h+d) \cdot \varepsilon_{tu} \cdot E_{frpt} + 2 \cdot \rho_{frpc} \cdot h \cdot \varepsilon_{tu} \cdot \frac{y-d'}{h-y} = 0 \tag{15}$$

where:

$$\phi = El \cdot \frac{(1-\alpha)}{(\beta-1)} \tag{16}$$

and where ε_{tu} and σ_{tu} represent respectively the limit traction strain and stress for wood and ε_{cu} and σ_{cu} the corresponding limit compressive strain and stress.
Once that neutral axis position is found, it is possible to proceed to the calculation of the ultimate bending moment of the section, which can be expressed as follows:

$$Mu = F_I \cdot b_I + \frac{2}{3} \cdot F_{II} \cdot y \cdot (1-k) + \frac{2}{3} \cdot F_{III} \cdot (h-y) + F_{IV} \cdot (h-y) + F_V \cdot (y-d) \tag{17}$$

2.3 Analysis of different failure mechanisms

As has been shown in section 2.2, equations (3)-(17) lead, neglecting failure of the FRP reinforcements, to two different failure mechanisms. The first one involves the possibility of wood traction stress attainment, while the other occurs when the limit compression stress is reached. Experimental tests have shown that the most frequent failure mechanism is the one in which traction failure occurs with or without

partial plasticization of the compressed zone, both for unreinforced wood elements as well as reinforced wood elements.
The solutions of equation (15) seem to more adequately represent the mechanical behavior of a wood element, at least for wood of low quality (high presence of defects).
Under this configuration, the neutral axis position in a reinforced wood beam moves downward for increasing values of the elastic modulus and area fraction, as shown in figure 3.
Analyzing the distribution of forces over the entire section, it is possible to state that reinforcement with FRP materials applied in a traction zone is very useful in improving the ultimate bending moment through the contribution of force F_{IV}. Furthermore, this reinforcement allows greater strain in the compression region thanks to the greater distance of the compressed fibers from the neutral axis.
This kind of intervention may be used for wood having poor mechanical characteristics due to the presence of defects, such as wood elements in which the difference between ultimate traction stress and ultimate compressive stress is negligible.
Theoretically, a high value of fraction area in the traction region should cause an inversion of the failure mechanism. Figure 3 shows a change in the slope of the lines that represent the normalized position of the neutral axis on a section versus the elastic modulus of the fiber. The two circles in figure 3 indicate the transition between the two failure mechanisms.

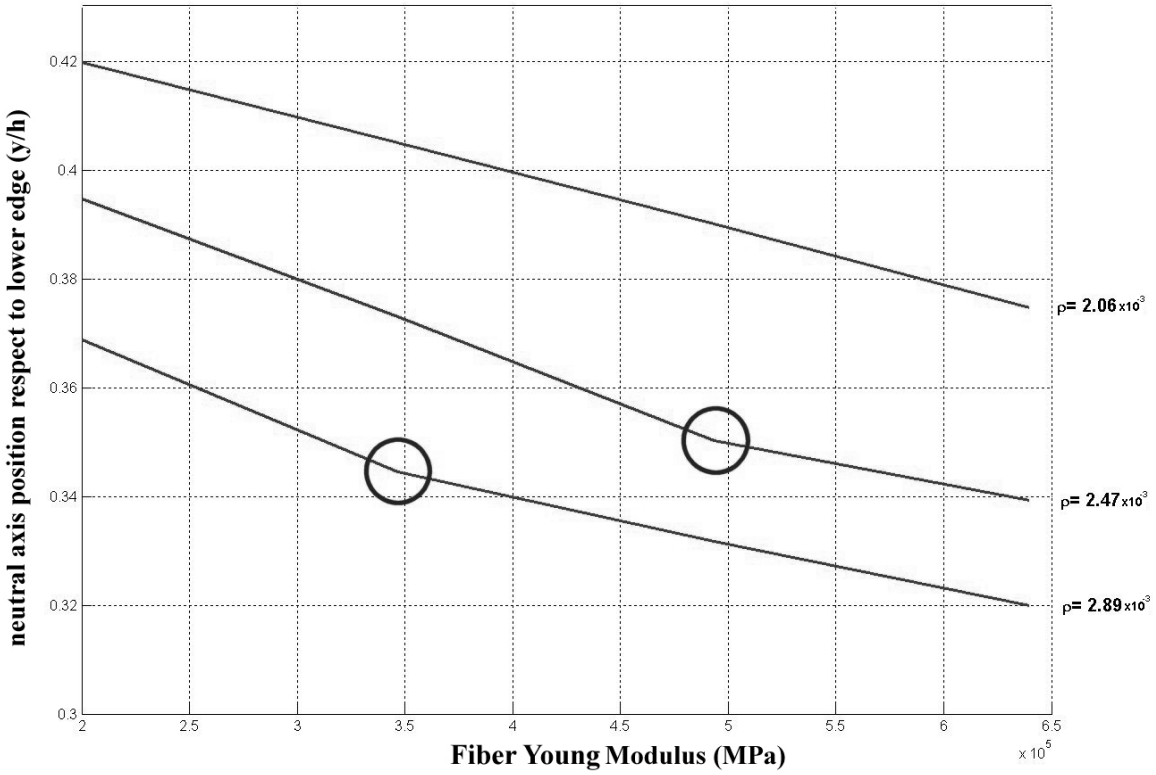

Figure 3. Neutral axis position of a wood beam reinforced with thin fiber sheets on lower side vs fiber elastic modulus and area fraction.

Several experimental tests (Triantafillou, 1997) showed that the most frequent mechanism is caused by the failure of the traction zone without the complete plasticization of the compression region, depending on the quality of the wood.
However, under particular conditions it is possible to note the other failure mechanism, which is theoretically preferable for several reasons. First, the section shows a more ductile behavior, while the stresses in the FRP material with reinforcement on both upper and lower edges of the section are highly increased and the composite material is therefore more involved.
Instead when wood elements reach a high degree of plasticization in the compression zone, the forces F_I, F_{II} e F_{III} may assume high values. However the centre of gravity of forces F_I and F_{II} moves downward causing a decrease of the offset of internal forces (figure 4).

Forces F_{IV} e F_V, generated by FRP reinforcements, allow an increase in the ultimate moment, as shown in figure 4b.

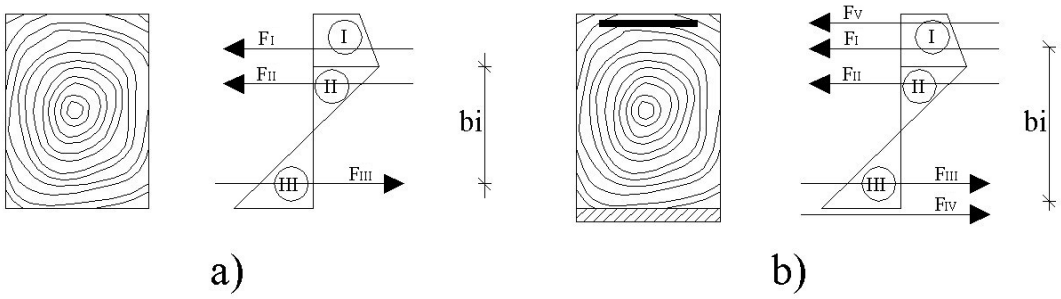

Figure 4 FRP reinforcement effect on a wood section under bending loads.

The situation changes when the wood element does not show significant plastic behavior. In this case the application of composite material in the compression zone causes an upward displacement of the neutral axis position.

The failure mechanisms described in this paper do not take into account the presence of defects and the non-homogeneity of wood. Therefore, an accurate calibration of the numerical procedure is required. This can be achieved with an adequate reduction of the ultimate traction resistance of wood depending on the wood quality. Then, a statistical approach becomes a necessary element in order to apply the non-linear method in the common design process of FRP reinforcement for wood elements.

Equations (3)-(17) can be easily extended to other cases in which different failure mechanisms are involved.

Another important aspect regards the possibility of using equations (3)-(17) to design FRP reinforcements involving pre-tension systems of FRP sheets. In fact, as with concrete elements, it is possible to take this effect into account through a pre-tension initial strain in the FRP sheets, ε_{pi}, equal to the ratio between initial stress in a sheet and the corresponding elastic modulus of the composite material. Then, strain in the sheet will be increased by ε_{pi}. It is clear that in this situation it is important to take into account the possible failure of the FRP sheets.

Equations (3)-(17) have been used to implement a numerical procedure for the calculation of the ultimate moment of a rectangular wood section reinforced with FRP elements. The following paragraph will show results obtained from an experimental campaign on wood beams with FRP reinforcements, which were used to calibrate and validate the numerical procedure.

3. FLEXURAL TESTING

A series of CFRP-reinforced beams was designed with varying area fractions of the fiber reinforcement. The un-reinforced solid wood beams were reinfoced with a continuous carbon fabric overlay and a Mac MBrace epoxy matrix. The MBrace epoxy resin consisted of two parts of Saturant A and B which were mixed in a ratio of 3:1 by volume, as required for the standard of Mac products. The study examined the use of Carbon FRP sheets and bars. For each reinforcement material, two or three different fiber reinforcement area fractions were evaluated in the testing program and properties of the two composite materials (sheets and bars) are shown in Tables 1 and 2. The CFRP sheets were characterized following ASTM D 3039 specifications.

The mechanical characterization of the CFRP bars was carried out on 9 samples. The CFRP bars were tested in traction using a dynamometer type Controls 70-C810/B. Tests were executed in load control with a velocity of 30 MPa sec^{-1}. The end of each sample was inserted into a metal cylinder and connected to the bars with an epoxy resin. The metal cylinders were necessary in order to not damage the CFRP bars by the compression stresses induced by the loading shoes of the dynamometer.

Primary fiber and volume fraction	-
Actual diameter	7.5mm
Number of samples tested	9
Mean tensile strength	1053MPa
Strength standard deviation	41.22MPa
Mean strain at failure	0.69percent
Modulus of elasticity	151030MPa

Table 1. Results of traction tests (CFRP bars).

Dry fiber thickness t	0.165mm
Number of samples tested	10
Mean tensile strength	3388MPa
Strength standard deviation	271MPa
Mean strain at failure	1.00percent
Strain standard deviation	0.09percent
Modulus of elasticity	417625MPa

Table 2 Results of traction tests (CFRP monodirectional sheets).

3.1 Experimental procedure

Twenty timber beams 4000mm long with a cross section of 200x200mm were used for the experimental program. All the beams were surveyed for both their geometric dimensions and wood defects. With regard to the classification of timber reported in Giordano (1964), these beams were classified in the second category.

After an 18-month seasoning period the tests were executed. Following each test, two samples were extracted from the failure zone in order to measure the humidity ratio. The geometric survey together with the values of the weight of the beams permitted the determination of the wood weight density. The average value of the humidity ratio was 10.88percent (with a standard deviation of 1.32percent), while that of the timber density was 453.6kg/m^3 (with a standard deviation of 37.69kg/m^3).

Tests were executed under four-point bending. The simply supported span between the two bearings, made of two semi-cylindrical metal elements (diameter 609mm), was 3600mm. The load span was equal to 1200mm. The beams were loaded with a 245kN MTS actuator and a spreader beam. The spreader beam, centered about the midspan, created a 1200mm zone with constant moment and zero shear. The vertical displacements of the beams were measured using 6 inductive trasducers. Two more channels of acquisition were used for the measurement of the time and the load.

Two tests were executed on each beam: a first test for the evaluation of the stiffness and a second for the evaluation of the flexural capacity. The Young modulus of wood was measured by recording the load-deflection behavior of all beams between two load levels. In fact the test for the Young modulus for the timber beams is a non-destructive test. The beams were loaded in four-point bending following the same scheme used for capacity evaluation tests. Six loading and unloading cycles were executed between the load values of P=11kN and P=40kN. Load was applied at a stroke-controlled rate of ±80kN per minute. The stiffness was calculated for each loading cycle using the values of the mid-span deflection obtained by averaging the two LVDT readings at each side of each beam. Loads for the measurement of the flexural capacity of the wood beams were applied monotonically to failure. The test for the evaluation of the flexural capacity was executed at a stroke-controlled rate of 7mm per minute to achieve failure in 10 to 15 minutes.

3.2 Un-reinforced beams

Three un-reinforced wood beams were tested in order to find their flexural capacity. The results for the un-reinforced beams are reported solely for the purpose of quantitatively evaluating the effectiveness of the interventions through a comparison with the results for strengthened beams.

Their flexural capacity was found to be 51.12kN, 69.39kN and 96.39kN respectively for beams Nos. 12, 17 and 19. The load-deflection behavior of the un-reinforced beams is shown in Fig. 6. The initial load-deflection behavior was linear until wood yield in compression and crushing occurred. After yielding, the beam behaved non-linearity with a reduced stiffness up to failure. The observed mode of failure was due to cracking of the timber. The average failure load for the three beams was 72.35kN.

3.3 Beams reinforced with CFRP sheets

The first set of specimens included 8 full scale beams of varying reinforcement ratios, ρ: specifically, 0.082 and 0.123percent. Three different reinforcement schemes with CFRP sheets were evaluated in the testing program:

1. two 3400x100mm CFRP sheets bonded centrally to the tension zone of the beams (ρ= 0.082 percent) (beams Nos. 1, 16, 14) (Figure 5a);
2. three 3400x100mm CFRP sheets bonded centrally to the tension zone of the beams (beams Nos. 9, 15) (ρ= 0.123percent) (Figure 5a)
3. two couples of two 3400x100mm CFRP sheets bonded laterally to the tension zone of the beams (beams Nos. 4, 6, 7) (ρ= 0.082percent) (Figure 5b)

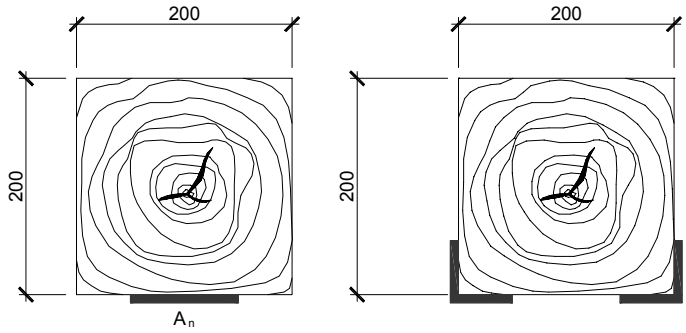

(a) (b)

Figure 5. Different schemes for CFRP sheet reinforcement.

The gluing of the sheets must be prepared very carefully. First, the wood surface must be even, un-weathered and clean. This can be also achieved by planing the surface until sound wood is reached, particularly at the ends of the sheets, to ensure a proper anchoring. The wood surface must be dry at the time of gluing and the gluing surface of the CFRP sheets must be degreased and clean.

The load-deflection behavior of un-strengthened timber beams and that of beams strengthened with 2 CFRP sheets are shown in Figure 6. Failure occurred at a load level of 92.23kN and 113.69kN respectively for beams Nos. 1 and 16. Therefore, the reinforcing scheme increased the capacity (maximum load) by 42.3percent in comparison to the values measured for the un-reinforced wood beams.

With regard to schemes 2 and 3, the CFRP reinforcement caused an increase in the average maximum load at failure varying from 55.0 to 60.3percent. The presence of CFRP sheets seems to arrest crack opening, confines local rupture and bridges local defects in the timber. The result is that the timber can support higher loads before failure. Moreover, as can be observed from the load-deflection curves, there is a significant decrease in scattering of the results, as a consequence of the quoted crack opening arrest.

The influence of the two experimental variables (reinforcement ratio and fiber type) on the wood beam failure loads and deformations are also shown in Figures 6 and 7. Initially the load defection is shown to be linear elastic up to local failures induced by the presence of defects (knots, etc.). Wood yield produced a non-linear response terminated by a sudden drop of the load as a result of CFRP rupture. CFRP rupture was immediately followed by wood fracture in the tension zone, resulting in collapse of the beams. The wood beams reinforced with CFRP sheets revealed more ductile behavior with respect to un-reinforced beams.

One of the principal focuses of this investigation was on the load deformation characteristics of the fiber-reinforced wood beams. The presence of the carbon sheets causes an interesting increase in stiffness varying from 22.5 to 30.3percent compared to that of the same wood beams before reinforcement (Table 3).

Type of Strengthening	Wood beams q.ty	Maximum Load [kN]	Maximum Load Increment [percent]	Stiffness Increment [percent]
Scheme 1	3	102.96	42.3	22.5
Scheme 2	2	115.96	60.3	29.2
Scheme 3	2	112.16	55.0	30.3

Table 3: Results of flexion tests (CFRP sheet reinforcement).

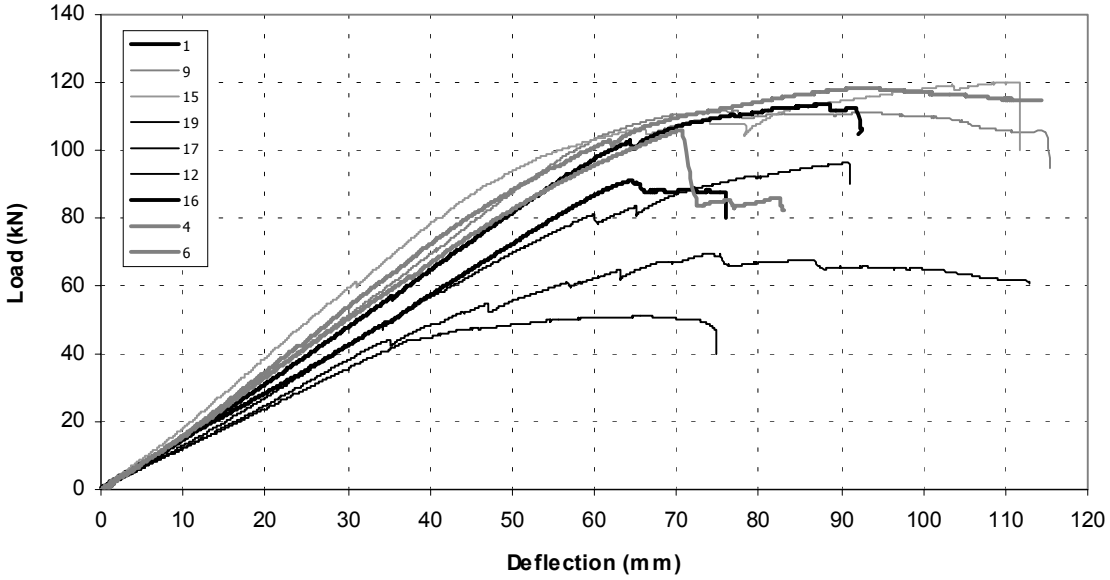

Figure 6. Load-Deflection curves for CFRP sheet reinforcement (Nos. 12, 17, 19: un-reinforced beams; Nos. 1,16: scheme 1 reinforcement; Nos. 9,15: scheme 2 reinforcement; Nos. 4, 6: scheme 3 reinforcement).

3.4 Beams reinforced with CFRP pre-stressed sheets

A pre-stressing force was applied to 4 wood beams in order to increase the stiffness properties of the reinforced beams. The pre-stressing operations were effected using a three-point bending test over a span of 3600mm in which the wood beam was loaded up to the mid-span deflection of 30 mm. This deflection value corresponds to a load of approx. 20-25kN equal to 25-35percent of the ultimate wood flexion load. The reinforcement was applied in the compression zone. The wood beam remained under this bending load for all the duration of the reinforcing operation and of reinforcement curing for a minimum of 7 days.

Two wood beams were reinforced with two CFRP sheets (scheme No. 1) and two beams with three CFRP sheets (scheme No. 2)

Reinforced beams were tested in flexion with four-point bending as described in section 3.1. The reinforcement, now placed in the tension zone, never debonded from the wood surface. The flexural capacity of the four beams reinforced according to scheme No.1 and scheme No.2 was similar to the one obtained for the beams reinforced without the pre-stressing operations. The increase in stiffness was equal to 27.7percent and 24.8percent for the beams reinforced according to schemes Nos. 1 and 2 when a comparison was made with the same beams before reinforcement (Table 4, Figure 7). These results differ widely from those obtained in a previous experimental study carried out on small wood samples (Borri et al., 2002). In fact, in these samples, significant increases in stiffness were found. However it must be considered that the small wood samples were without defects (knots, etc.) and the pre-stressing value could be greater, therefore resulting more effective. The presence of defects, typical for full-scale wood beams, causes significant decreases in ultimate flexion capacity and the value of applicable pre-stressing is limited.

Type of strengthening	Wood beams q.ty	Maximum Load [kN]	Maximum Load Increment [percent]	Stiffness Increment [percent]
Scheme 1	2	110.26	52.4	27.7
Scheme 2	2	104.03	43.8	24.8

Table 4: Results of flexion tests (pre-stressed sheets).

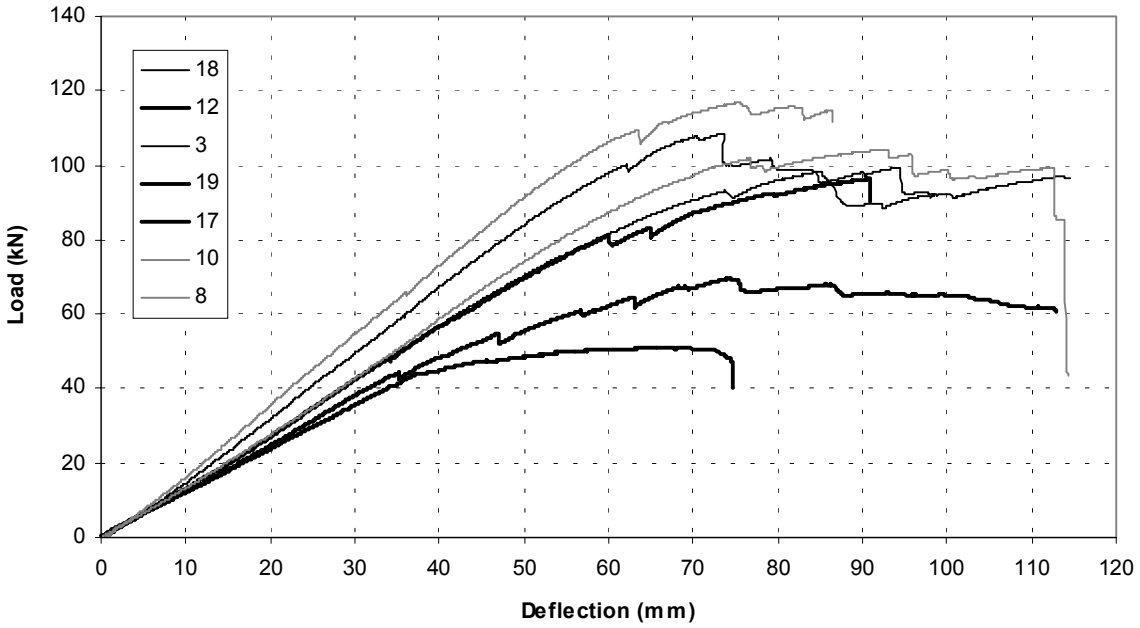

Figure 7 Load-Deflection curves for CFRP pre-stressed sheet reinforcement (Nos. 12, 17, 19: un-reinforced beams; Nos. 8, 10: scheme 1 reinforcement; Nos. 3,18: scheme 2 reinforcement).

3.5 Beams reinforced with CFRP bars

Five wood beams were strengthened with CFRP bars. Load versus deflection diagrams are plotted in Figure 8. One or two grooves (dimensions 20x10x3600 mm) were cut in each beam in the tension zone as indicated in Figure 9. The depth of the groove was 20 mm and the bars were bonded to the wood by the same epoxy-resin used as a matrix for the sheets. The resin cured for 7 days at room temperature before testing. Smoothing the surface of the beam completed the application process.

All the beams tested revealed less ductile behavior compared to that of both the un-reinforced beams as well as those reinforced with CFRP sheets. Table 4 summarizes the experimental results for the five beams tested, including the maximum loads and the corresponding stiffness increment compared with the same beams before reinforcement application. The CFRP reinforcement caused an increase in the average maximum load at failure from 72.35kN to 109.99kN, which represents an increase of 52percent (Table 5). The load deflection curves in Figure 8 show that the beams exhibited a more essentially linear behavior up to failure. Wood yield is interrupted from beam failure due to the appearance of cracks. The positive effect induced by the presence of the bars is not able to confine local ruptures and bridge local defects. Moreover, the grooves cut in the beams in order to insert the CFRP bars produce some limited damage.

Type of Strengthening	Wood beams q.ty	Maximum Load [kN]	Maximum Load Increment [percent]	Stiffness Increment [percent]
1 CFRP bar	2	93.27	28.9	22.0
2 CFRP bars	2	109.99	52.0	25.5
2 CFRP bars (pre-stressed)	1	102.96	42.3	30.3

Table 5: Results of flexion tests (bar reinforcement).

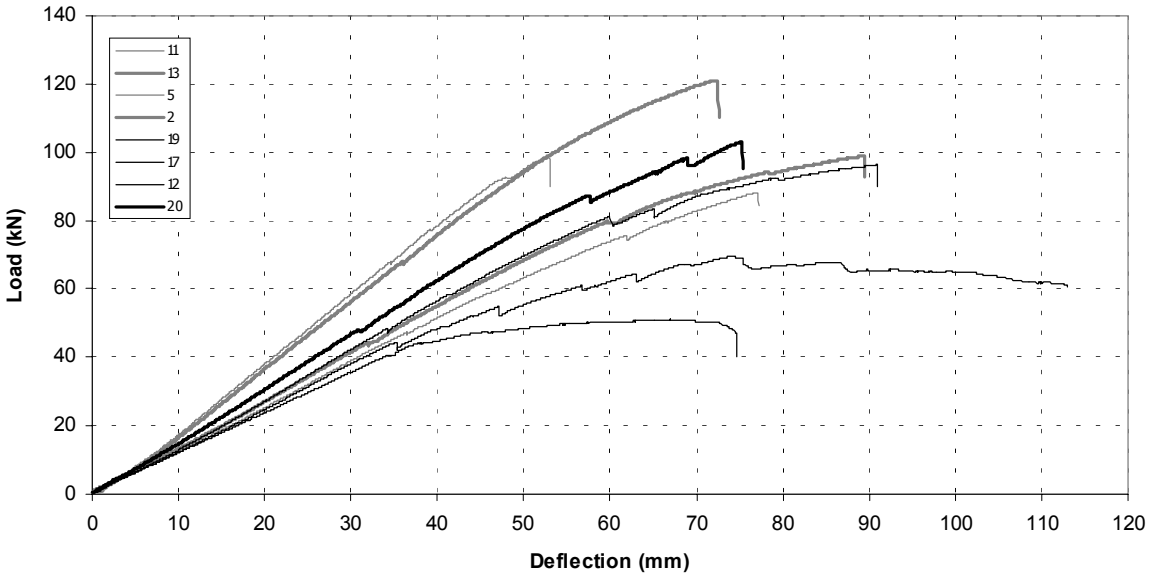

Figure 8. Load-Deflection curves for CFRP bar reinforcement (Nos. 12, 17, 19: un-reinforced beams; Nos. 5, 11: one-bar reinforcement; Nos. 2, 13: two-bar reinforcement; No. 20: reinforcement with two pre-stressed bars).

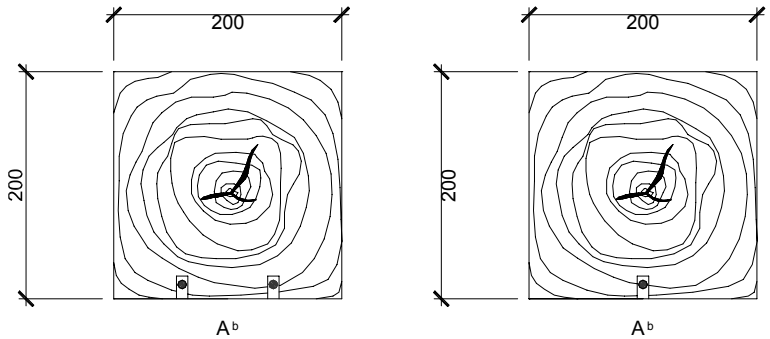

Figure 9: Different schemes for CFRP bar reinforcement.

4. EXPERIMENTAL COMPARISON

Following the experimental tests the equations (3)-(17) were applied to develop a numerical procedure which can be used to estimate the failure load.

The critical point of the numerical procedure consists in the selection of the most adequate characteristic values for wood limit stresses.

This step was carried out using values found in other studies and from the comparison of the values obtained from the failure loads of the un-reinforced beams. In addition, a series of simulations with a Finite Element Method program were executed to support the calibration process. Figure 10 shows the typical distribution of a reinforced wood element under failure load. In the upper part of the element it is possible to see the compressed zone which is completely plasticized.

Table 6 shows a synthesis of failure load values obtained either from experimental results or numerical estimation. Once that numerical model is calibrated, differences between experimental failure loads and estimated failure loads are negligible.

Reinforcement type	Experimental failure load [kN]	Numerical failure load [kN]	Error [percent]
2-sheet reinforcement	102.96	106	2.95
3-sheet reinforcement	115.96	111	4.28
1-bar reinforcement	93.27	97	4.00
2-bar reinforcement	108.03	104	3.73

Table 6.

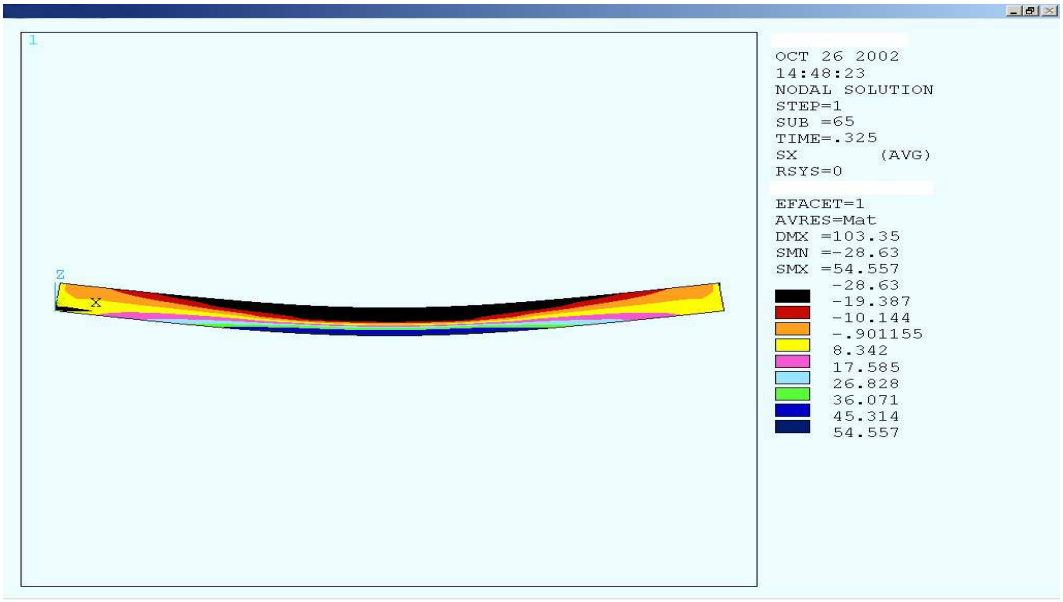

Figure 10. Normal stress distribution in a FRP reinforced wood element at the failure load.

5. CONCLUSIONS

The strengthening of wood structural elements through innovative techniques presents numerous interesting aspects. The results of the experiments carried out, although varying according to the tests performed, have highlighted the limitations as well as the advantages of the various techniques.

The use of CFRP as a strengthening technique can be applied without necessitating the removal of the overhanging part of the structure. The technique used proved to be easy and fast to execute, even when on in situ parts. In particular, it demonstrated to be very promising in many cases of reinforcement of old, historical structural wood parts.

Mechanical tests on the reinforced wood showed that external bonding of FRP sheets on the side loaded in tension produces very interesting effects. In the case of three layers of carbon fibers, which demonstrated to be the most highly performing configuration, results showed increases in flexural capacity up to 60.3percent compared to un-reinforced beams. The use of CFRP bars as a reinforcing method produced smaller increases in capacity. However, taking into account that CFRP bars are inserted into wood beams and are not visible, this type of intervention demonstrated to be of interest. With regard to the increase in stiffness, results are less relevant. Maximum increases did not exceed 30percent when compared to values measured for un-reinforced beams.

It has then been demonstrated that it is not possible to obtain a further increase in the stiffness by pre-loading the wood beams. Gluing the composite reinforcement while the wood beams were under a flexion load applied in the direction opposite to that used during the tests, produced a maximum stiffness increase of as much as 27.7percent, similar to the value obtained for simply-reinforced beams.

The numerical procedure developed on the basis of the Bazan-Buchanan law has shown that it is possible to estimate the failure loads of a FRP reinforced wood element. More specifically, the non-linear analysis permits a clearer perspective of the effect of FRP reinforcement on a wood beam. This is especially useful for the designer who needs a simple tool to select the most suitable kind of reinforcement. From the point of view of limit analysis, this method will be useful in providing more consistent design tools for these interesting reinforcing techniques.

6. REFERENCES

Bazan, I. M. M. (1980). Ultimate bending strength of timber beams:- PhD thesis. Nova Scotia Technical College. Halifax. Nova Scotia. Canada..

Biblis, E. J. (1965). Analysis of wood-fiberglass composite beams within and beyond the elastic region.'. Forest Prod. J.. 15(2).81-88.

Blom, A. e Backlund, J. (1980). "Composite materials reinforcement at cutouts in laminated timber beams" Res. Rep., Dept. of Mech. Engrg., Linkoping Institute of Technology, Svezia.

Bodig, J.. e Jayne. B. (1982). Mechanics of wood and wood composites. Van Nostrand Reinhold. New York. N. Y.

Bohannan, B. (1962). "Prestressed wood members." Forest Prod. J. 12(12). 596-602.

Borgin, K. B., Loedolff. G. F. e Saunders. G. R. (1968). "Laminated wood beams reinforced with steel strips." J. Struct. Engrg.. ASCE, 94(7).1681-1705.

Borri, A., Corradi, M. e Speranzini, E. (2001). Travi in legno rinforzate con barre o con tessuti in fibra di carbonio, *L'Edilizia*, editrice De Lettera, 8-9, agosto-settembre, anno XV, Milano, 48-56.

Borri, A., Corradi, M. e Vignoli, A. (2002). New materials for strengthening and seismic upgrading interventions, International Workshop Ariadne 10, Arcchip, April 22-28 2002, Prague, Czech Republic, cd-rom, 1-24.

Buchanan, A. H. (1986). "Combined bending and axial loading in lumber." J. Struct. Engrg., ASCE, 112(12), 2592-2609.

Buchanan, A. H. (1990). "Bending strength of lumber." J. Strucl. Engrg., ASCE, 116(5), 1213-1229.

Bulleit, W. M., Sandberg, L. B., e Woods, G. J. (1989). "Steel-reinforced glued laminated timber." J. Strucl. Engrg., ASCE, 115(2), 433-444.

Coleman, G. E. e Hurst, H. T. (1974). "Timber structures reinforced with light gage steel." Forest Prod. J., 24(7), 45-53.

Dziuba, T. (1985). "The ultimate strength of wooden beams with tension reinforcement." Holzforschung und Holzverwertung, 37(6), 115-119.

Giordano, G. (1964). "La moderna tecnica delle costruzioni in legno", Hoepli, Milano

Giuriani, E. e Frangipane, A. (1993), "Wood-to-concrete composite section for stiffening of ancient wooden beamfloors", I Workshop Italiano sulle Costruzioni Composte -Trento, 307-317.

Giuriani, E., Plizzari, G.A. e Bassini, C. (1999), "Experimental results on masonry wall anchored ties", in STREMAH99, Dresda (Germania), Giugno 1999, 55-64.

Hallstrom, S. (1995). "Glass fibre reinforcement around holes in laminated timber beams" Rep. No. 95-14, Dept. of Lightweight structures., Royal Institute of Technology, Stoccolma, Svezia.

Hoyle, R. J. (1975). "Steel-reinforced wood beam design." Forest Prod. J., 25(4), 17-23.

Hull, D. (1981). An introduction to composite materials. Cambridge Univ. Press, Cambridge, England.

Iyer, S. L.. Sivaramakrishnan, C. e Atmaran, S. (1989). "Testing of reinforced concrete bridges for external reinforcement." Proc. Sessions Related to Struct. Mater., Structures Congress '89, ASCE, 116-122.

Kaiser, H. (1989). "Strengthening of reinforced concrete with epoxy-bonded carbon-fiber plastics," PhD thesis, ETH, Zurich, Switzerland.

Kropf, F.W. e Meierhofer, U. (2000) "Strengthening, Retrofitting and Upgrading of Timber Structures with High-Strength Fibres",SEI 3/2000

Kobetz, R. W. e Krueger, G. P. (1976). "Ultimate strength design of reinforced timber: Biaxial stress failure criteria." Wood Sci. , 8(4), 252-262.

Krueger, G. P. (1973). "Ultimate strength design of reinforced timber: State of the art." Wood Sci., 6(2), 175-186.
Krueger, G. P. e Eddy, F. M. (1974). "Ultimate strength design of reinforced timber: Moment-rotation characteristics." Wood Sci., 6(4), 330-344.
Krueger, G. P. e Sandberg, L. B. (1974). "Ultimate strength design of reinforced timber: Evaluation and design parameters." Wood Sci. , 6(4), 316-330.
Lantos, G. (1970). "The flexural behavior of steel reinforced laminated timber beams." Wood Sci. , 2(3), 136-143.
Larsen, H.J., Gustafsson, P.J. and Enquist, B. (1992). "Tests with glass-fibre reinforcement of wood perpendicular to the grain" Rep. TVSM-7067, Dept. of Mech. Engrg., Lund Institute of Technology, Svezia.
Meier, U. (1987). "Bridge repair with high performance composite materials." Material and Technik, 4,125-128.
Mitzner, R. C. (1973). "Durability and maintenance of plywood overlaid with fiberglass reinforced plastic." Res. Report No.119, part 3, Am. Plywood Assoc., Tacoma. Wash.
Peterson, J. (1965). "Wood beams prestressed with bonded tension elements" J. Struct. Engrg., ASCE, 91(1), 103-119.
Plevris, N. e Triantafillou, T.C. (1992) "FRP Reinforced wood as structural material", Journal of materials in Civil Engineering, ASCE, Vol.4, 3:300-315.
Ronca, P., Gelfi, P. e Giuriani, E. (1991). "The behavior of a wood-concrete composite beam under cyclic and long term load", in STREMAH91, Seville, Spain, 1:263-275.
Sliker, A. (1962). "Reinforced wood laminated beams." Forest Prod. J., 12(1),91-96.
Triantafillou, T. C. e Plevris, N. (1991). "Post-strengthening of r/c beams with epoxy-bonded fiber-composite materials." Proc. ASCE Specialty Conf. on Advanced Composites for Civ. Engrg. Strucl. , ASCE, 245-256.
Triantafillou, T. C. e Deskovic. N. (1991). "Innovative prestressing with FRP sheets: Mechanics of short-term behavior." J. Engrg. Mech., ASCE, 117(7), 1652-1672.
Triantafillou, T. C., (1997). "Shear reinforcement of wood using FRP materials" J. Materials in Civil Engrg., ASCE, 9(2), 65-69.

Acknowledgements

Thanks go to Mac S.p.A. for their technical assistance during the strengthening operations.